JOURNAL OF Materials Chemistry Communication

# Ca-doped $RCoO_3$ (R = Gd, Sm, Nd, Pr) as thermoelectric materials

Ji-Woong Moon,*[a] Won-Seon Seo,[a] Hiroki Okabe,[b] Takasi Okawa[b] and Kunihito Koumoto[a]

[a]*Department of Applied Chemistry, Graduate School of Engineering, Nagoya University, Nagoya 464-8603, Japan. E-mail: jiwoongmoon@hotmail.com*
[b]*Daiken Chemical Co. Ltd., Osaka 536-0011, Japan*

***Received 17th May 2000, Accepted 28th June 2000***
***Published on the Web 7th August 2000***

**The electrical resistivity and Seebeck coefficient of $(R_{0.9}Ca_{0.1})CoO_3$ (R = Gd, Sm, Nd, Pr) rapidly decrease with increasing ionic radius of the rare-earth element, and the Seebeck coefficients (p-type) are fairly high at low temperatures and attain low and constant values at high temperatures; $(Pr_{0.9}Ca_{0.1})CoO_3$ shows the highest figure-of-merit, $1.3 \times 10^{-4}$ $K^{-1}$ at 85 °C, although this rapidly decreases with temperature above 300 °C due to the decreasing Seebeck coefficient and increasing electronic thermal conductivity.**

Thermoelectric materials with high energy conversion efficiencies, such as PbTe, $Bi_2Te_3$, *etc.*, are easily oxidized, decompose, or melt at high temperatures in an air atmosphere.[1–4] Though SiGe alloys are comparatively stable up to fairly high temperatures and are currently used above 700 °C, the environment for their use is usually limited to vacuums or inert atmospheres.[5] Doped $FeSi_2$[6] is another such material which is oxidation resistant, even at 700 °C in air, but its thermoelectric properties are still unsatisfactory. In recent years, increasing attention has been given to oxides as thermoelectric materials because of their high thermal stability and oxidation resistance, and non-toxicity. Several systems have been investigated, such as $(ZnO)_5In_2O_3$,[1–4] $CdIn_2O_4$,[7] $In_2O_3$–$SnO_2$,[8] $(Zn_{1-x},Al_x)O$,[9] $(Ba,Sr)PbO_3$,[10] $(La,Sr)CrO_3$,[11] $(Ca,M)MnO_3$ (M = Bi, In),[12] $Ca_9Co_{12}O_{28}$,[13] and Li-doped NiO.[14] However, the values of figure-of-merit, $Z$ ($Z = S^2\sigma/\kappa$, where $S$, $\sigma$, and $\kappa$ are the Seebeck coefficient, electrical conductivity, and thermal conductivity, respectively), of such oxides are smaller than those of alloys and semiconductors. Recently, it has been reported that $NaCo_2O_4$[15] has a high figure-of-merit ($8.8 \times 10^{-4}$ $K^{-1}$), but its application seems to be limited because of the volatility of sodium above 800 °C. Therefore, it is necessary to further investigate new oxide materials with both high performance and environmental stability.

Rare-earth cobalt oxides, $RCoO_3$ (R = rare-earth element), have been extensively studied because of their interesting electrical and magnetic properties.[16,17] The electrical conduction mechanism and the observed metal–insulator (M–I) transition have been reported for many years.[18–21] Some rare-earth cobalt oxides, such as $GdCoO_3$[20,21] and $NdCoO_3$[18,19,21] *etc.*, show fairly high Seebeck coefficients in the vicinity of room temperature and were expected to have unique thermoelectric properties. Although there have been a lot of studies on rare-earth cobalt oxides focused on their electronic transport mechanism, studies on their applicability to thermoelectric materials have been scare. In the present study, the electrical conductivity, Seebeck coefficient, and thermal conductivity of partially Ca-doped oxides, $(R_{0.9}Ca_{0.1})CoO_3$ (R = Gd, Sm, Nd, Pr), were measured as functions of temperature, and their thermoelectric figures-of-merit were evaluated.

Starting powders of $R_2O_3$, $CaCO_3$, and $Co_3O_4$ (R = Gd, Sm, Nd, Pr; all 99.9% purity, Kojundo Chemicals Laboratory) were weighed in specific proportions to obtain the compositions of $(R_{0.9}Ca_{0.1})CoO_3$ and were mixed in a ball mill for 24 h using zirconia balls and ethanol. The mixed powders were dried and calcined at 1000 °C for 10 h in air. After cooling, they were crushed with a mortar and pestle. The powders were compacted under an isostatic pressure of 196 MPa, and then sintered at 1100 °C for 10 h in air. X-Ray diffraction (RINT-2100, Rigaku) measurements of the synthesized powders were performed using Cu-Kα radiation with a Ni filter. The specimens for electrical measurements were cut out of the sintered bodies into rectangular bars of 4 mm × 4 mm × 12 mm with a diamond saw. The heads of two Pt–Pt 13%Rh thermocouples were embedded in drilled holes at the ends of each specimen and were fixed in place with platinum wires. Electrical conductivity was measured by the DC four-probe technique, using each Pt leg of the thermocouple as a current lead. For thermopower measurement, the temperature gradient in the specimen was generated by passing cooling air through an alumina protection tube over one end of the specimen. The temperature difference between the two ends was controlled to 2–15 K by varying the flow rate of the air. Thermopower measured as a function of temperature difference gave a straight line and the Seebeck coefficient was calculated from its slope. Thermal diffusivity and specific heat were measured by the laser flash method (ULVAC-TC3000V) and differential scanning calorimetry (DSC; Mac Science DSC3200S), respectively. Thermal conductivity was calculated from the product of density, thermal diffusivity, and specific heat.

The X-ray diffraction patterns of $(R_{0.9}Ca_{0.1})CoO_3$ (R = Gd, Sm, Nd, Pr) powders calcined at 1000 °C can be indexed on the basis of JCPDS cards of $RCoO_3$ (R = Gd, Sm, Nd, Pr), where $GdCoO_3$ and $SmCoO_3$ have orthorhombic, and $NdCoO_3$ and $PrCoO_3$ have cubic perovskite-type structures, respectively. Fig. 1 shows the electrical conductivities of the $(R_{0.9}Ca_{0.1})CoO_3$ samples measured in the temperature range 100–900 °C. The electrical conductivity at the same temperature increased with the increasing ionic radius of the rare-earth element (Pr > Nd > Sm > Gd). $(Gd_{0.9}Ca_{0.1})CoO_3$ and $(Sm_{0.9}Ca_{0.1})CoO_3$ showed semiconducting behavior over the whole temperature range examined, *i.e.* the electrical conductivity increased with increasing temperature. Similar behavior was observed for $(Pr_{0.9}Ca_{0.1})CoO_3$ and $(Nd_{0.9}Ca_{0.1})CoO_3$ up to 700 and 800 °C, respectively. However, when the temperature exceeded *ca.* 700 °C, semi-metallic behavior was observed for $(Pr_{0.9}Ca_{0.1})CoO_3$ and $(Nd_{0.9}Ca_{0.1})CoO_3$. A similar change from semiconducting to metallic behavior was also observed for $(Sm_{0.9}Ca_{0.1})CoO_3$ when the temperature exceeded 900 °C (data are not presented). The formation of oxygen vacancies and their contribution to electrical conductivities were not taken into consideration because the amount of $Ca^{2+}$ substitution for $R^{3+}$ in this work is thought to be relatively small[22] and electrical conductivities were fairly high in all cases.

Fig. 2 shows the Seebeck coefficient, $S$, of $(R_{0.9}Ca_{0.1})CoO_3$ as a function of temperature. The sign of the Seebeck coefficient was positive over the entirety of the temperature range measured; *i.e.* the major conduction carriers are holes. At low temperatures (in the vicinity of 100 °C), the absolute values

DOI: 10.1039/b003964k

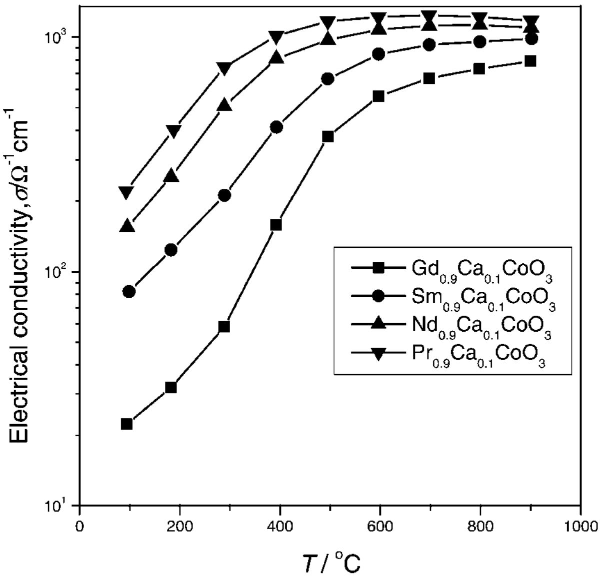

**Fig. 1** Electrical conductivity of $R_{0.9}Ca_{0.1}CoO_3$ (R = Gd, Sm, Nd, Pr) as a function of temperature.

of the Seebeck coefficients for all compositions are fairly high, but become lower and constant at high temperatures, indicating a metallic nature. The Seebeck coefficient of $(Gd_{0.9}Ca_{0.1})CoO_3$ increased slightly with increasing temperature, went through a maximum at *ca.* 200 °C, and then decreased. In contrast, for $(Sm_{0.9}Ca_{0.1})CoO_3$, $(Nd_{0.9}Ca_{0.1})CoO_3$, and $(Pr_{0.9}Ca_{0.1})CoO_3$, the Seebeck coefficients monotonically decreased with increasing temperature. It can be clearly seen that the Seebeck coefficient decreases with the increasing ionic radius of the rare-earth element. This tendency is the complete opposite of that shown by the electrical conductivity, but is an understandable phenomenon if the relationship between electrical conductivity and Seebeck coefficient for a normal semiconductor is taken into consideration; a larger electrical conductivity by means of a higher carrier density usually gives rise to a smaller Seebeck coefficient.

As far as the temperature dependences of the electrical conductivity and Seebeck coefficient are concerned, M–I transition appears to be favored by rare-earth elements with larger ionic radii (Pr > Nd > Sm > Gd) and occurs at lower temperatures. This phenomenon can be explained by a model[22,23] based on Zaanen, Sawatzky, and Allen's (ZSA)[24,25] framework. The degree of distortion of the structure determines the onset of the electronic localization–delocalization transition. For a given $R^{3+}$ size, the $CoO_6$ octahedron is tilted in order to optimize R–O bond distances, giving rise to a deviation of the Co–O–Co angles from 180°, which determines the degree of overlapping of the cobalt 3d and oxygen 2p orbitals. Large rare-earth ions cause the Co–O–Co bonds to straighten out and become closer to 180°. The Co 3d and O 2p orbital overlap increases as the Co–O–Co angles become closer to 180°, and this structural change must give rise to the observed rare-earth element dependence of the electronic behavior of $RCoO_3$.

Fig. 3 shows the thermal conductivity, $\kappa$, of $(R_{0.9}Ca_{0.1})CoO_3$ as a function of temperature (100–700 °C). The overall $\kappa$ value of a solid is generally given as $\kappa = \kappa_{ph} + \kappa_{el}$, where $\kappa_{ph}$ and $\kappa_{el}$ are lattice and electron thermal conductivity, respectively. The thermal conductivity of $(Sm_{0.9}Ca_{0.1})CoO_3$, $(Nd_{0.9}Ca_{0.1})CoO_3$, and $(Pr_{0.9}Ca_{0.1})CoO_3$ monotonically increase with increasing temperature. In the case of $(Gd_{0.9}Ca_{0.1})CoO_3$, the change in $\kappa$ is negligible up to 300 °C, after which $\kappa$ increases with increasing temperature. Fig. 4 shows the electronic contribution ($\kappa_{el}$) to the total thermal conductivity ($\kappa$), estimated using the Wiedemann–Franz law, for $(Gd_{0.9}Ca_{0.1})CoO_3$ and $(Pr_{0.9}Ca_{0.1})CoO_3$. The thermal conductivity of small polarons is expected to be much less than is implied by the Wiedemann–Franz law, and $\kappa_{el}$ can be neglected in this regime.[26] Accordingly, the observed rapid decrease in $S$ and increase in $\sigma$ with increasing temperature, and the large electronic contribution to the thermal conductivity are all thought to be evidence of the transition from small polaron to large polaron conduction. Because of the small binding energy and large intersite transfer energy of a large polaron, the Wiedemann–Franz law can provide a reasonable upper limit for $\kappa_{el}$. For $(Pr_{0.9}Ca_{0.1})CoO_3$, the ratio $\kappa_{el}/\kappa$ monotonically increased with increasing temperature from *ca.* 0.10 at 100 °C to *ca.* 0.61 at 700 °C. The constant $\kappa$ region was observed only for $(Gd_{0.9}Ca_{0.1})CoO_3$ at temperatures below 300 °C, indicating that the conduction holes in this material are more strongly bound to the lattice.

Fig. 5 shows the temperature dependence of the figure-of-merit, $Z$. At low temperatures (in the vicinity of 100 °C), the $Z$ values of $(Sm_{0.9}Ca_{0.1})CoO_3$, $(Nd_{0.9}Ca_{0.1})CoO_3$, and $(Pr_{0.9}Ca_{0.1})CoO_3$ were larger than that of $(Gd_{0.9}Ca_{0.1})CoO_3$. $(Pr_{0.9}Ca_{0.1})CoO_3$ showed the largest value of $Z$,

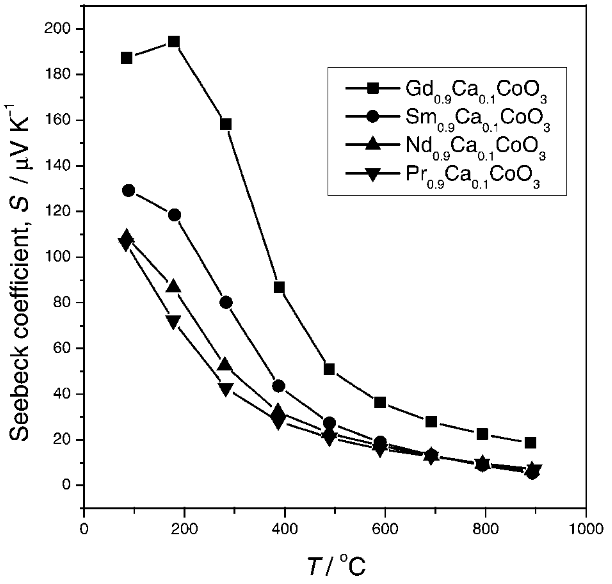

**Fig. 2** Seebeck coefficient of $R_{0.9}Ca_{0.1}CoO_3$ (R = Gd, Sm, Nd, Pr) as a function of temperature.

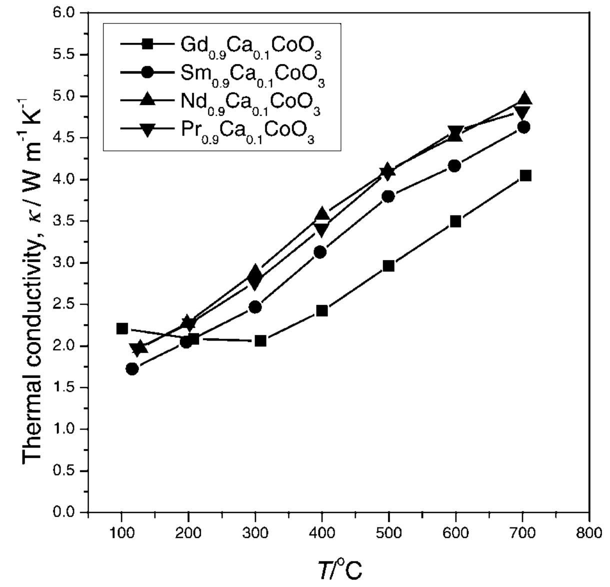

**Fig. 3** Thermal conductivity of $R_{0.9}Ca_{0.1}CoO_3$ (R = Gd, Sm, Nd, Pr) as a function of temperature.

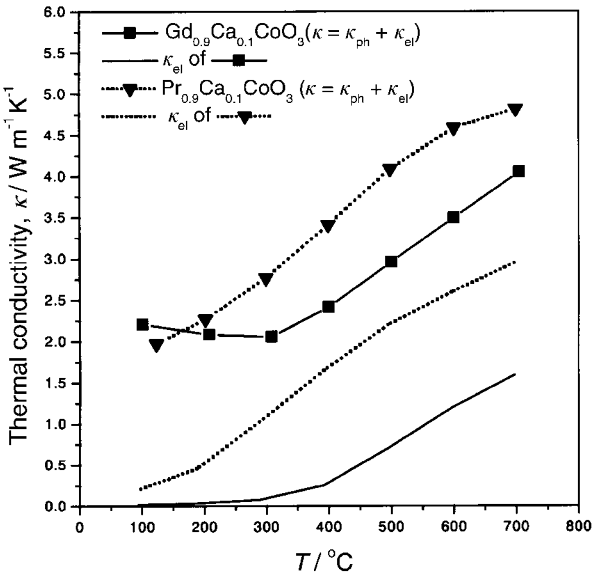

**Fig. 4** Electronic contribution to the thermal conductivity of $Gd_{0.9}Ca_{0.1}CoO_3$ and $Pr_{0.9}Ca_{0.1}CoO_3$ (estimated using the Wiedemann–Franz law).

$1.3 \times 10^{-4}$ $K^{-1}$, at 85 °C. Above 300 °C, $Z$ for $(Pr_{0.9}Ca_{0.1})CoO_3$ rapidly decreased with increasing temperature due to the decreasing Seebeck coefficient and increasing electronic thermal conductivity. In this temperature region (≧250 °C), $(Gd_{0.9}Ca_{0.1})CoO_3$ showed the largest values of $Z$. The $Z$ value of $(Gd_{0.9}Ca_{0.1})CoO_3$ gradually increased with increasing temperature and showed its maximum, $0.7 \times 10^{-4}$ $K^{-1}$, at 282 °C.

Compared with other p-type oxide thermoelectric materials, except $NaCo_2O_4$, the maximum figure-of-merit attained in the present study is fairly large, especially at low temperatures. Even for high temperature thermoelectric generation, materials with large figures-of-merit at low temperatures are favorable, because one side of the thermoelectric device is unavoidably exposed to a low temperature environment. It can be concluded from the present study that rare-earth cobalt oxides are potential candidate materials for thermoelectric energy conversion. Substitution of other rare-earth elements for R or doping aliovalent cations other than $Ca^{2+}$ is now under investigation in order to obtain better thermoelectric properties.

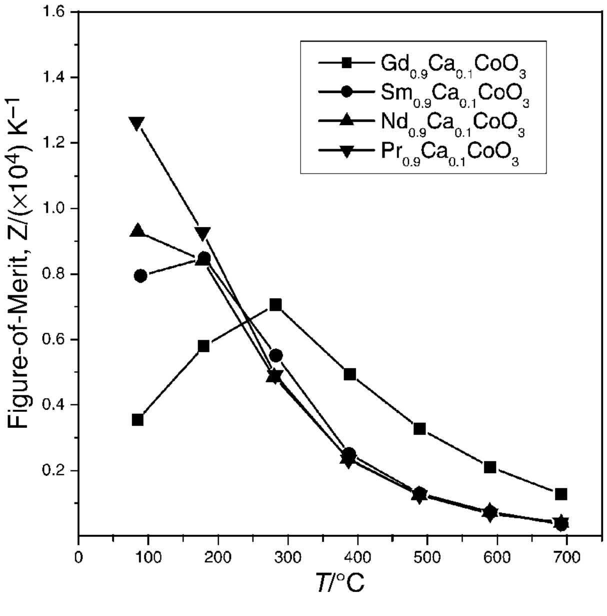

**Fig. 5** Figure-of-merit for $R_{0.9}Ca_{0.1}CoO_3$ (R = Gd, Sm, Nd, Pr) as a function of temperature.

## Acknowledgements

The authors thank Woosuck Shin, Noorimitsu Murayama, and Yukihiko Yamauchi of NIRIN (National Industrial Research Institute of Nagoya) for their assistance with the thermal diffusivity measurements.

## Notes and references

1 H. Ohta, W. S. Seo and K. Koumoto, *J. Am. Ceram. Soc.*, 1996, **79**(8), 2193.
2 H. Hiramatsu, H. Ohta, W. S. Seo and K. Koumoto, *J. Jpn. Soc. Powder Powder Metall.*, 1997, **44**(1), 44.
3 M. Kazeoka, H. Hiramatsu, W. S. Seo and K. Koumoto, *J. Mater. Res.*, 1998, **13**(3), 523.
4 Y. Masuda, M. Ohta, W. Pitschke, W. S. Seo and K. Koumoto, *J. Solid State Chem.*, 2000, **150**, 221.
5 F. D. Rosi, in *Modern Perspectives on Thermoelectrics and Related Materials*, ed. D. D. Allred, C. B. Vinning and G. A. Slack, *Mater. Res. Soc. Symp. Proc.*, Pittsburg, PA, 1991, vol. 234, p. 3.
6 T. Tokiai, T. Uesugi and K. Koumoto, *J. Am. Ceram. Soc.*, 1995, **78**, 1089.
7 R. D. Shannon, J. L. Gilson and R. J. Bouchard, *J. Phys. Chem. Solids*, 1977, **38**, 877.
8 M. Ohtaki, D. Ogura, K. Eguchi and H. Arai, *J. Mater. Chem.*, 1994, **4**, 653.
9 T. Tsubota, M. Ohtaki, K. Eguchi and H. Arai, *J. Mater. Chem.*, 1996, **6**, 1.
10 M. Yasukawa and N. Murama, *J. Mater. Sci. Lett.*, 1997, **16**, 1731.
11 W. J. Weber, C. W. Griffin and J. L. Bates, *J. Am. Ceram. Soc.*, 1987, **70**, 265.
12 M. Ohtaki, H. Koga, T. Tokunaga, K. Eguchi and H. Arai, *J. Solid State Chem.*, 1995, **120**, 105.
13 S. Li, R. Funahashi, I. Matsubara, K. Ueno and H. Yamada, *J. Mater. Chem.*, 1999, **9**, 1659.
14 W. Shin and N. Murayama, *Jpn. J. Appl. Phys.*, 1999, **38**, L1336.
15 I. Terasaki, Y. Sasago and K. Uchinokura, *Phys. Rev. B*, 1997, **56**, R12685.
16 P. M. Raccah and J. B. Goodenough, *Phys. Rev.*, 1967, **155**, 932.
17 V. H. Bhide, D. S. Rajoria, G. Ramma Rao and C. N. R. Rao, *Phys. Rev.*, 1972, **6**, 1021.
18 C. N. R. Rao, V. G. Bhide and N. F. Mott, *Philos. Mag.*, 1975, **32**, 1277.
19 C. N. R. Rao and O. M. Parkash, *Philos. Mag.*, 1977, **35**, 1111.
20 A. Casalot, P. Dougier and P. Hagenmuller, *J. Phys. Chem. Solids*, 1971, **32**, 407.
21 D. S. Rajoria, V. G. Bhide, G. Rama Rao and C. N. R. Rao, *J. Chem. Soc., Faraday Trans. 2*, 1973, **70**, 512.
22 G. Ch. Kostogloudis, N. Vasilakos and Ch. Ftikos, *Solid State Ionics*, 1998, **106**, 207.
23 J. B. Torrance, P. Lacorre, A. I. Nazzal, E. J. Ansaldo and Ch. Niedermayer, *Phys. Rev. B*, 1992, **45**, 8209.
24 J. Zaanen, G. A. Sawatzky and J. W. Allen, *Phys. Rev. Lett.*, 1995, **55**, 418.
25 J. Zaanen, G. A. Sawatzky and J. W. Allen, *J. Solid State Chem.*, 1980, **88**, 8.
26 J. L. Cohn, J. J. Neumeier and C. P. Popovviciu, *Phys. Rev. B*, 1997, **56**, R8465.